ELECTRONIC SUPPLEMENTARY INFORMATION

In-silico design of novel NRR electrocatalysts: cobalt-molybdenum alloys

Blanca Castellano-Varona,[a] Moussab Harb,[b] Javier Araña,[a] Luigi Cavallo*[b]
and Luis Miguel Azofra*[a]

[a]Instituto de Estudios Ambientales y Recursos Naturales (i-UNAT), Universidad de Las Palmas de Gran Canaria (ULPGC), Campus de Tafira, 35017, Las Palmas de Gran Canaria, Spain.
E-mail: luismiguel.azofra@ulpgc.es
[b]KAUST Catalysis Center (KCC), King Abdullah University of Science and Technology (KAUST), Thuwal 23955-6900, Saudi Arabia.
E-mail: luigi.cavallo@kaust.edu.sa

---

1. COMPUTATIONAL DETAILS

The mechanism for the N_2 adsorption and its electrochemical conversion into NH_3 has been studied by means of density functional theory (DFT) through the generalised gradient approximation (GGA) with the revised Perdew-Burke-Ernzerhof (RPBE) functional with Pade approximation,[1] using a plane-wave cut-off energy of 400 eV.[2,3] The Brillouin zone (periodic boundary conditions) was sampled by 3×3×1 *k*-points using the Monkhorst-Pack scheme. In order to avoid interactions between periodic slabs, a vacuum width of 15 Å was imposed. Optimisation calculations were done using energy and force convergence limits equal to 10^{-4} eV/atom and $|0.01|$ eV/Å, respectively. Due to the paramagnetic properties of the Co and CoMo catalysts, spin-polarised calculations were imposed in all cases. Over these optimised structures, vibrational frequencies were calculated over Γ point in order to obtain zero-point energies (ZPE), thermal corrections, and entropy contributions. At this step, explicit dispersion correction terms to the energy were also employed through the use of the D3 method with the standard parameters programmed by Grimme and co-workers.[4,5] All optimisation and vibrational frequency calculations have been performed throughout the facilities provided by the Vienna *Ab-Initio* Simulation Package (VASP, version 5.4.4).[6–9]

2. DFT CHARACTERISATION OF COBALT SLABS

The experimental crystal structure of hcp cobalt (ε-Co) [and fcc (γ-Co)] unit cell was taken and treated with Materials Studio. The unit cell was expanded and truncated to conform a slab of 125 Co atoms (Co_{125}) constituted by five layers or 25 Co atoms by each layer and being terminated with a (001) surface for ε-Co [(111) for γ-Co]. Due to the paramagnetic properties of the cobalt catalyst, spin-polarised considerations were imposed during optimisation. Different local spin magnetic moments for Co atoms were tested in order to correctly define magnetisation, and therefore energetic properties of the material. At RPBE functional level, magnetic moments for Co atoms have been calculated as 1.761, 1.685, 1.653, 1.685, and 1.761μ, for the first, second, third, fourth and fifth layers, respectively. These parameters have been used as initial magnetic moments for Co atoms during the NRR modelling ($\mu = 0$ for N and H atoms).

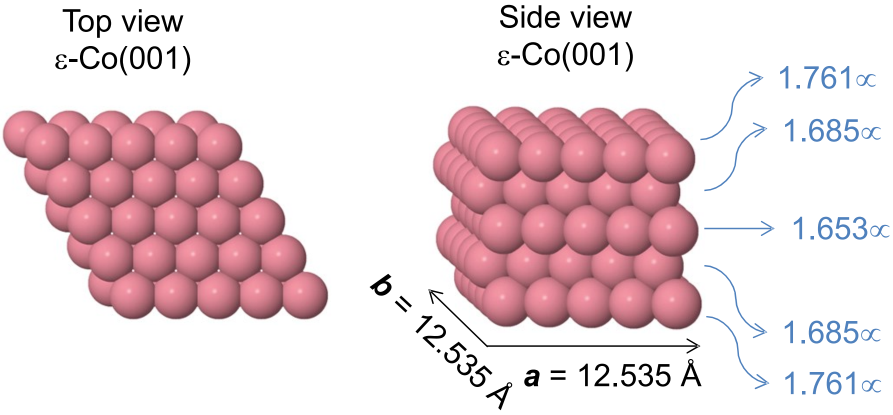

Figure S1. Top and side views of ε-Co_{125}(001) slab model together with the optimised lattice parameters and magnetic moments at RPBE level of functional.

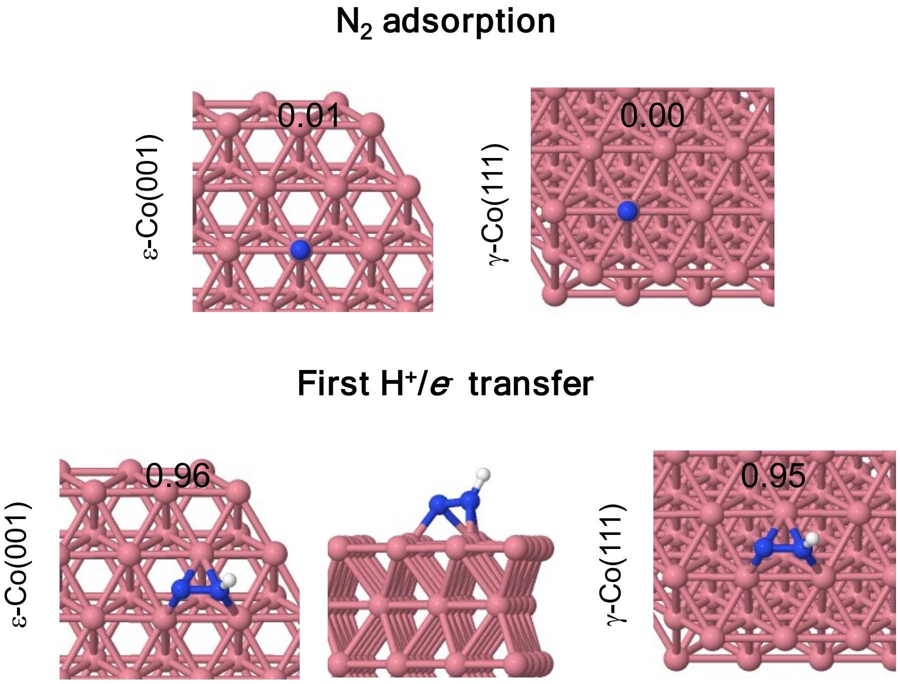

Figure S2. Interaction of both N_2 and N_2H species with the ε-Co(001) and γ-Co(111) surfaces. Free energies are shown in eV.

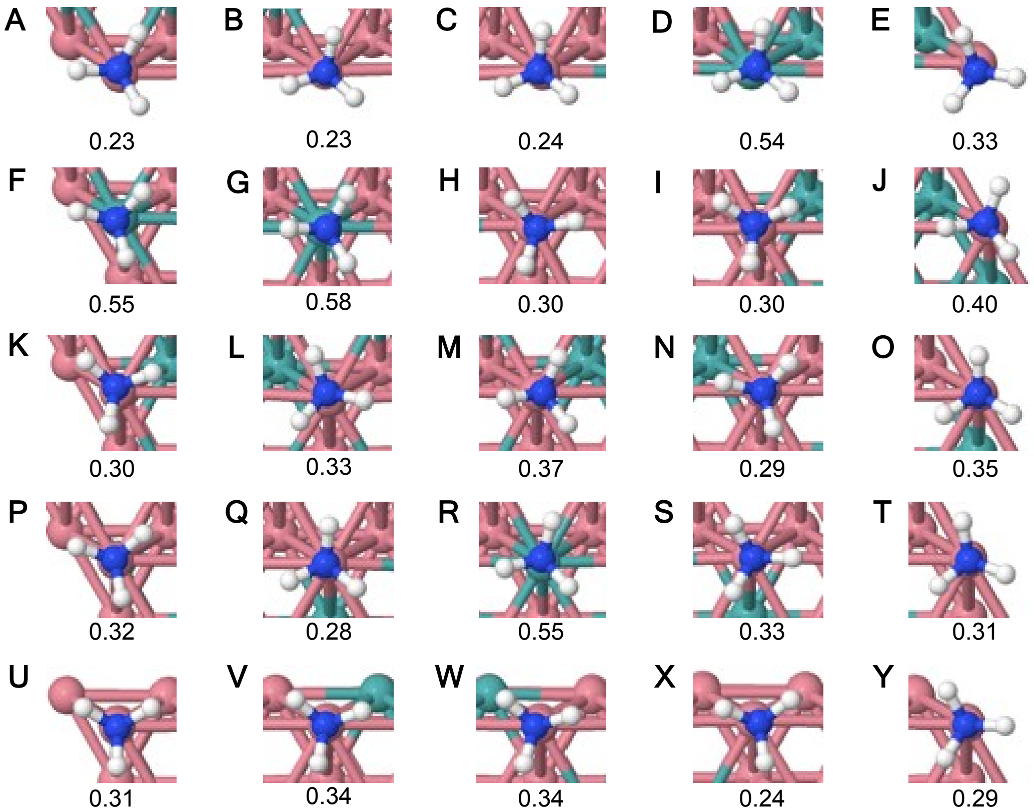

Figure S3. Adsorbed NH_3 species at different points of the (001) surface in the CoMo alloy. Free desorption energies are shown in eV. (See labels' meaning at Fig. 4 in the manuscript).

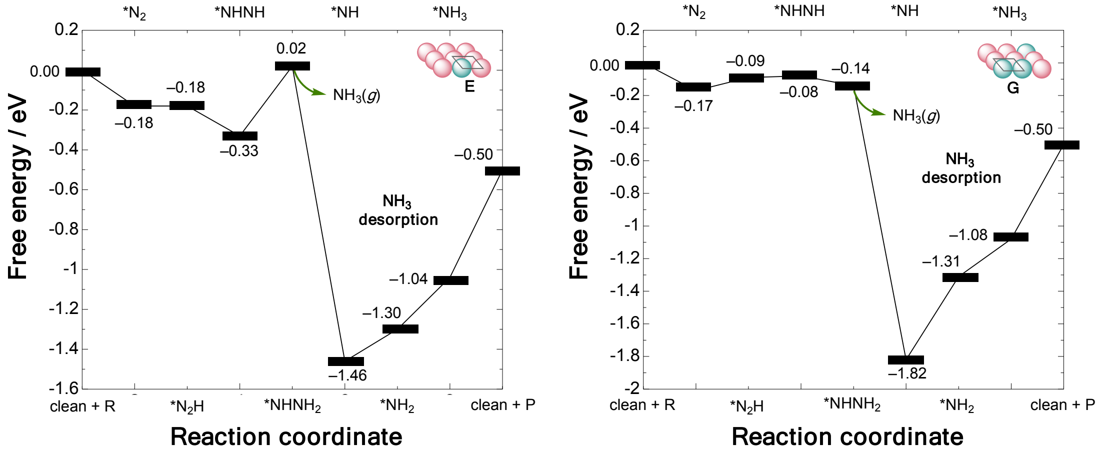

Figure S4. Free reaction energy profiles for NRR catalysed by CoMo(001) at **E** and **G** active sites. (See labels' meaning at Fig. 4 in the manuscript). Free energies are shown in eV at RTP conditions when there is not applied bias ($U = 0$ V) and pH = 0 (CHE).

3. MODELLING PERFORMANCE

Once ε-Co_{125}(001) slab was properly optimised, the NRR mechanism was investigated by optimising the different states during N_2 conversion. All Co atoms of this (001) surface are equivalent. Once N_2 is adsorbed on the catalytic surface ($*N_2$), a set of six H^+/e^- pair transfers occur; the first one leads to $*N_2H$, the second one to $*NHNH$ or $*NNH_2$, and so on up to balance the chemical equation:

$$N_2(g) + 6\ H^+ + 6\ e^- \rightleftharpoons 2\ NH_3(g)$$

During optimisation, no structural constrains have been applied. Over the optimised geometries, vibrational frequencies were calculated in order to obtain zero-point energies (ZPE), thermal corrections, and entropy contributions. In such cases, all metal atoms were frozen during vibrational frequency calculations, imposing no constrain on N and H atoms. At this stage, explicit D3 dispersion corrections were also applied.

4. THERMOCHEMISTRY

DFT calculations have been performed using the revised PBE (RPBE) functional, which offers a better estimation of the reaction energy for hydrogenation of N_2 into ammonia than the classical PBE one: –0.50 eV (RPBE) *vs*. –0.34 eV (experimental). Free energy calculations have been carried out as follows:

$$G = E + \int C_P\, dT - TS$$

where G, E and C_P refer to the free energy, electronic energy, and heat capacity, respectively.

The entropy term can be expressed as the sum of the translational, rotational, vibrational and electronic contributions as follows:

$$S = S_t + S_r + S_v + S_e$$

Finally, intrinsic zero-point energy (ZPE) and extrinsic dispersion (D) corrections were included to obtain this expression:

$$G = E + \int C_P\, dT - T(S_t + S_r + S_v + S_e) + \mathrm{ZPE} + D$$

Since $S_e \approx 0$ at the fundamental electronic level, Table S1 gathers the thermodynamic quantities for N_2, H_2 and NH_3 gases at standard conditions (298.15 K of temperature, 1 bar of fugacity for all gases).

Table S1. Thermodynamic quantities, in eV, for N_2, H_2 and NH_3 gases at standard condition (298.15 K, $f = 1$ bar) using RPBE functional.

Gas	***E*(+*D*)**	**$\int C_P\, dT$**	**–*TS***	**ZPE**	***G***
$N_2(g)$	–16.24	0.09	–0.59	0.15	–16.60
$H_2(g)$	–6.98	0.09	–0.40	0.27	–7.02
$NH_3(g)$	–19.47	0.11	–0.62	0.91	–19.08

In the case of solids and adsorbates, some approximations can be assumed:

1. As for gases, at the fundamental electronic level $S_e \approx 0$.
2. Translational and rotational motions can be neglected, therefore, $S_t \approx 0$ and $S_r \approx 0$. In this sense, all entropy contributions come from vibrations: $S = S_v$. Similarly, translational and rotational contributions to the heat capacity are neglected.

Therefore, free energies for the different states along NRR have been calculated as to:

$$G = E + \int C_P\, dT - TS_v + \mathrm{ZPE} + D$$

5. PROTON-COUPLED ELECTRON TRANSFER (PCET) APPROACH

The reaction free energy between two states along the N_2 capture/conversion process carried out *via* electrochemical approach, *i.e.*, $N_2(g) + 6\ H^+ + 6\ e^-(aq) \rightleftharpoons 2\ NH_3(g)$, can be expressed, by applying the proton-coupled electron transfer (PCET) approach,[10] as to:

$$\Delta G_R = G({*}N_{2-m}H_{n-3m}) + mG(NH_3) - G(*) - G(N_2) - nG(H^+/e^-)$$

where '*' denotes the surface material, n is the number of H^+/e^- pairs transferred and m the number of NH_3 molecules released, if applicable ($m = 0, 1$). Obviously, for $n = m = 0$, the reaction free energy leads to the binding free energy:

$$\Delta G_b = G({*}N_2) - G(*) - G(N_2)$$

In this regard, all energy values have been referred using the computational hydrogen electrode (CHE) model for the H^+/e^- transfer, considering the chemical potential of the H^+/e^- pair in aqueous solution as the half of the H_2 gas molecule at standard hydrogen electrode (SHE) conditions, *i.e.*, $f(H_2) = 1$ bar, $U = 0$ V, and pH = 0, being $f(H_2)$ and U the fugacity of H_2 and the external potential applied, respectively.

$$\mu(H^+/e^-) = \tfrac{1}{2}\,\mu\,(H_2)$$

And therefore, ΔG_R can be expressed as to:

$$\Delta G_R = G(*N_{2-m}H_{n-3m}) + mG(NH_3) - G(*) - G(N_2) - n/2\ G(H_2)$$

REFERENCES

1 B. Hammer, L. B. Hansen and J. K. Nørskov, *Phys. Rev. B*, 1999, **59**, 7413–7421.

2 P. E. Blöchl, *Phys. Rev. B*, 1994, **50**, 17953–17979.

3 G. Kresse and D. Joubert, *Phys. Rev. B*, 1999, **59**, 1758–1775.

4 S. Grimme, J. Antony, S. Ehrlich and H. Krieg, *J. Chem. Phys.*, 2010, **132**, 154104.

5 S. Grimme, S. Ehrlich and L. Goerigk, *J. Comput. Chem.*, 2011, **32**, 1456–1465.

6 G. Kresse and J. Hafner, *Phys. Rev. B*, 1993, **47**, 558–561.

7 G. Kresse and J. Hafner, *Phys. Rev. B*, 1994, **49**, 14251–14269.

8 G. Kresse and J. Furthmüller, *Phys. Rev. B*, 1996, **54**, 11169–11186.

9 G. Kresse and J. Furthmüller, *Comput. Mater. Sci.*, 1996, **6**, 15–50.

10 A. A. Peterson, F. Abild-Pedersen, F. Studt, J. Rossmeisl and J. K. Nørskov, *Energy Environ. Sci.*, 2010, **3**, 1311–1315.